Bulg. J. Phys. **38** (2011) 175–183

Cylindrical or Spherical Dust-Ion Acoustic Shocks in an Adiabatic Dusty Plasma

B. Sahu

Department of Mathematics, West Bengal State University, Barasat, Kolkata-700126, India

Received *18 April 2011*, Revized *30 June 2011*

Abstract. Using the reductive perturbation technique, the nonplanar cylindrical and spherical modified Burgers' equations are derived for dust ion acoustic waves in an unmagnetized dusty plasma, whose constituents are adiabatic ion fluid, Boltzmann electrons and negatively charged static dust particles. The solution of modified Burgers' equations in nonplanar geometry is numerically analyzed. The properties of dust ion acoustic waves in nonplanar cylindrical and spherical geometry are investigated. It has been found that the nonplanar geometry effects have a very significant role in the formation of shock waves. We have also reduced the modified Burgers' equation to an ordinary nonlinear differential equation using the Lie algebraic method. The numerical solution of these equations is given for two values of η_0, the viscosity parameter.

PACS codes: 52.35.Fp, 52.27.Lw, 52.35.Tc

1 Introduction

By now the study of dusty plasmas has become a popular topic of research. This is because of the ubiquitous presence of dusty plasmas in interstellar clouds, cometary environments and planetary rings [1-3]. Dusty plasmas are also of importance in laboratory devices, industrial processes and Earth's environment [4-8]. It may be noted here that dusty plasma supports two types of acoustic modes: high frequency ion acoustic mode involving mobile ions and static grains, and a low frequency dust acoustic wave involving mobile dust grains. Both modes have been observed in experiments [9-10]. A particular field of study which has received a lot of attention is that of solitary waves and shock waves. Shukla and Silin [11] have investigated the existence of dust ion acoustic waves, which are the normal modes of unmagnetized collisionless dusty plasmas of infinite extent. The dust ion acoustic shock wave (DIASW) was observed by Nakamura *et al.* [12-13] in a collisional dominated dusty plasma. They have shown that both monotonic and oscillatory shock waves exist and the dust density has vital role on the shock waves and phase velocity of the wave. The propagation of DIASWs in dusty plasma has been studied by several authors [14-16]. Very recently Rahman *et al.* [17] have studied dust ion acoustic shock waves in dusty plasma considering ion-fluid temperature in planar geometry. They have shown that the effects of ion fluid temperature significantly modify the basic properties of DIASWs. However all these studies are limited to one-dimensional planar geometry which might not be a realistic situation for laboratory devices, since the DIASWs that might be observed in low-temperature dusty plasma discharges might not necessarily be bounded in one space dimension. There are cases of particular interest in which the assumption of planar geometry does not make any sense and one should work in the nonplanar geometries, specially cylindrical and spherical. The examples of nonplanar geometries of practical interest are capsule implosion (spherical geometry), shock tube(cylindrical geometry), star formation and supernova explosions, *etc*. It would be more realistic situation in laboratory and space plasmas, if we consider the nonplanar geometry instead of planar geometry. In recent years, several authors [18-22] have theoretically investigated the properties of dust ion acoustic and dust acoustic solitary waves in nonplanar geometry. The results show that the properties of solitary waves in bounded nonplanar geometry are very different from those in unbounded planar geometry, and a stationary propagation of cylindrical/spherical soliton no longer exists. This motivated us to study DIASWs in an adiabatic dusty plasma in bounded nonplanar cylindrical and spherical geometry. In this paper Burgers equation is numerically investigated in cylindrical and spherical geometry for DIASWs considering adiabatic ion fluid, Boltzmann electrons, and static dust particles. Here the dust charge variation is not taken into account [23] as it is found to be small for small amplitude solitary waves. Numerically we have studied the effects of plasma parameters on the propagation of DIASWs in cylindrical and spherical geometry. The organization of the paper is as follows. In Section 2 the basic equations are given and cylindrical and spherical Burgers' equations are derived. In Section 3 numerical results and discussion are given. Section 4 is kept for conclusion.

2 Basic Equations and Derivation of Cylindrical and Spherical Burgers' Equations

We consider an unmagnetized plasma comprising of adiabatic ion fluid, static negatively charged dust fluid and Boltzmann distributed electrons. The normalized fluid equations in such a dusty plasma system in cylindrical and spherical geometry are

$$\frac{\partial n_i}{\partial t} + \frac{1}{r^\nu}\frac{\partial}{\partial r}(r^\nu n_i u_i) = 0, \tag{1}$$

$$n_i\frac{\partial u_i}{\partial t}+n_iu_i\frac{\partial u_i}{\partial r}=-n_i\frac{\partial\phi}{\partial r}-\alpha\frac{\partial p_i}{\partial r}+\eta_in_i\Big[\frac{1}{r^\nu}\frac{\partial}{\partial r}\Big(r^\nu\frac{\partial u_i}{\partial r}\Big)-\frac{\nu u_i}{r^2}\Big], \quad (2)$$

$$\frac{\partial p_i}{\partial t}+u_i\frac{\partial p_i}{\partial r}+3p_i\frac{1}{r^\nu}\frac{\partial}{\partial r}(r^\nu u_i)=0, \quad (3)$$

$$\mu\exp(\phi)-n_i+(1-\mu)=0, \quad (4)$$

where $\nu=0$, for one-dimensional geometry and $\nu=1$, 2 for cylindrical and spherical geometry, respectively. In the above equations, n_i is the ion number density normalized by its equilibrium value n_{i0}, u_i is the ion fluid speed normalized by $C_i=(k_BT_e/m_i)^{1/2}$, ϕ is the wave potential normalized by k_BT_e/e, p_i is the ion thermal pressure normalized by $n_{i0}k_BT_i$, $\alpha=T_i/T_e$, $\mu=n_{e0}/n_{i0}$. The time and space variables are normalized by reciprocal plasma frequency ${\omega_{Pi}}^{-1}=(m_i/4\pi n_{i0}e^2)^{1/2}$ and the Debye length $\lambda_D=(k_BT_e/4\pi n_{i0}e^2)^{1/2}$, respectively and η_i is the viscosity coefficient of ion fluid normalized by $\omega_{Pi}\lambda_D^2$. We have assumed the quasineutrality condition in equation (4).

To derive the cylindrical and spherical Burgers' equations we use the stretched coordinates

$$\xi=\epsilon^{1/2}(r-v_0t)\quad\text{and}\quad\tau=\epsilon^{3/2}t\,. \quad (5)$$

We can express (1)–(4) in terms of ξ and ϵ as

$$\epsilon^{3/2}\frac{\partial n_i}{\partial\tau}-v_0\epsilon^{1/2}\frac{\partial n_i}{\partial\xi}+\epsilon^{1/2}\frac{\partial}{\partial\xi}(n_iu_i)+\frac{\nu\epsilon^{3/2}}{v_0\tau\Big(1+\dfrac{\epsilon\xi}{v_0\tau}\Big)}(n_iu_i)=0, \quad (6)$$

$$\begin{aligned}\epsilon^{3/2}n_i\frac{\partial u_i}{\partial\tau}-v_0\epsilon^{1/2}n_i\frac{\partial u_i}{\partial\xi}+\epsilon^{1/2}n_iu_i\frac{\partial u_i}{\partial\xi}&=-\epsilon^{1/2}n_i\frac{\partial\phi}{\partial\xi}-\epsilon^{1/2}\alpha\frac{\partial p_i}{\partial\xi}\\&+\epsilon^{1/2}\eta_0n_i\left[\epsilon\frac{\partial^2u_i}{\partial\xi^2}+\frac{\nu\epsilon^2}{v_0\tau\Big(1+\dfrac{\epsilon\xi}{v_0\tau}\Big)}\frac{\partial u_i}{\partial\xi}-\frac{\nu\epsilon^3}{v_0^2\tau^2\Big(1+\dfrac{\epsilon\xi}{v_0\tau}\Big)^2}u_i\right], \quad (7)\end{aligned}$$

$$\begin{aligned}&\epsilon^{3/2}\frac{\partial p_i}{\partial\tau}-v_0\epsilon^{1/2}\frac{\partial p_i}{\partial\xi}+\epsilon^{1/2}u_i\frac{\partial p_i}{\partial\xi}\\&\quad+3p_i\left[\epsilon^{1/2}\frac{\partial u_i}{\partial\xi}+\frac{\nu\epsilon^{3/2}}{v_0\tau\Big(1+\dfrac{\epsilon\xi}{v_0\tau}\Big)}u_i\right]=0, \quad (8)\end{aligned}$$

$$\mu(1+\phi+\frac{1}{2}\phi^2+\cdots)+(1-\mu)=n_i, \quad (9)$$

where $\eta=\epsilon^{1/2}\eta_0$ is assumed.

The dependent variables are expanded as follows:

$$n_i = 1 + \epsilon n_i^{(1)} + \epsilon^2 n_i^{(2)} + \cdots , \tag{10}$$

$$u_i = \epsilon u_i^{(1)} + \epsilon^2 u_i^{(2)} + \cdots , \tag{11}$$

$$p_i = 1 + \epsilon p_i^{(1)} + \epsilon^2 p_i^{(2)} + \cdots , \tag{12}$$

$$\phi = \epsilon \phi^{(1)} + \epsilon^2 \phi^{(2)} + \cdots . \tag{13}$$

Substituting (10)–(13) into (6)–(9), we obtain from the lowest order in ϵ, $n_i^{(1)} = \mu\phi^{(1)}$, $u_i^{(1)} = \mu v_0 \phi^{(1)}$, $p_i^{(1)} = 3\mu\phi^{(1)}$, $v_0 = \sqrt{3\alpha + 1/\mu}$.
To next higher order in ϵ, we obtain a set of equations,

$$\frac{\partial n_i^{(1)}}{\partial \tau} - v_0 \frac{\partial n_i^{(2)}}{\partial \xi} + \frac{\partial}{\partial \xi}(n_i^{(1)} u_i^{(1)}) + \frac{\partial u_i^{(2)}}{\partial \xi} + \frac{\nu u_i^{(1)}}{v_0 \tau} = 0, \tag{14}$$

$$\begin{aligned} \frac{\partial u_i^{(1)}}{\partial \tau} - v_0 \frac{\partial u_i^{(2)}}{\partial \xi} + u_i^{(1)} \frac{\partial u_i^{(1)}}{\partial \xi} - v_0 n_i^{(1)} \frac{\partial u_i^{(1)}}{\partial \xi} + \alpha \frac{\partial p_i^{(2)}}{\partial \xi} \\ = -\frac{\partial \phi^{(2)}}{\partial \xi} - n_i^{(1)} \frac{\partial \phi^{(1)}}{\partial \xi} + \eta_0 \frac{\partial^2 u_i^{(1)}}{\partial \xi^2} , \end{aligned} \tag{15}$$

$$\frac{\partial p_i^{(1)}}{\partial \tau} - v_0 \frac{\partial p_i^{(2)}}{\partial \xi} + u_i^{(1)} \frac{\partial p_i^{(1)}}{\partial \xi} + 3\frac{\partial u_i^{(2)}}{\partial \xi} + 3p_i^{(1)} \frac{\partial u_i^{(1)}}{\partial \xi} + \frac{3\nu u_i^{(1)}}{v_0 \tau} = 0, \tag{16}$$

$$n_i^{(2)} = \mu \phi^{(2)} + \frac{1}{2}\mu[\phi^{(1)}]^2. \tag{17}$$

Combining equations (14)–(17), we get a modified Burgers' equation

$$\frac{\partial \phi^{(1)}}{\partial \tau} + \frac{\nu}{2\tau}\phi^{(1)} + A\phi^{(1)} \frac{\partial \phi^{(1)}}{\partial \xi} - C\frac{\partial^2 \phi^{(1)}}{\partial \xi^2} = 0, \tag{18}$$

where

$$A = \frac{12\mu^2\alpha + 3\mu - 1}{2\mu\sqrt{3\alpha + 1/\mu}}, \qquad C = \frac{\eta_0}{2}\,. \tag{19}$$

Putting $\phi^{(1)} = u/A$, the equation (18) is reduced to

$$\frac{\partial u}{\partial \tau} + \frac{\nu}{2\tau}u + u\frac{\partial u}{\partial \xi} - C\frac{\partial^2 u}{\partial \xi^2} = 0. \tag{20}$$

Analytical solution of equation (20) is not available. However, (19) can be reduced to an ordinary differential equation by the following similarity transformation suggested by Lie algebraic analysis [24] *viz.* $u = v/\xi, \eta = \xi/\tau^{j12}$. Then the equation (20) is reduced to for $\nu = 1$,

$$-2C\eta^2 \frac{d^2 v}{d\eta^2} + (2v\eta + 4C\eta - \eta^3)\frac{dv}{d\eta} + v\eta^2 - 2v^2 - 4Cv = 0 \tag{21}$$

and for $\nu = 2$,

$$-2C\eta^2 \frac{d^2 v}{d\eta^2} + (2v\eta + 4C\eta - \eta^3)\frac{dv}{d\eta} + 2v\eta^2 - 2v^2 - 4Cv = 0. \qquad (22)$$

3 Numerical Results and Discussion

Burgers' equation is numerically investigated for cylindrical and spherical geometry for describing the nonlinear propagation of the DIASWs in an unmagnetized dusty plasma. For planar geometry ($\nu = 0$), a stationary solution of the equation (18) has the following form :

$$\phi^{(1)} = \frac{V}{A}\left[1 - \tanh\left(\frac{V(\xi - V\tau)}{2C}\right)\right], \qquad (23)$$

where V is a constant velocity normalized by C_i. In nonplanar geometry an exact analytical solution of equation (18) is not possible. Therefore we solve equation (18) numerically. The initial condition that we have used in our numerical results is the form of the stationary solution (20) at $\tau = -10$. In Figure 1 we have plotted the shock wave structure evolved at $\tau = -5$ in different geometries for two values of η_0, the viscosity parameter. It is seen that shock height and shock steepness in different geometry are different from each other. The height and steepness of spherical shock wave are larger than that of the cylindrical shock wave, which is again larger than that of the one-dimensional shock wave. It should be noted that the structure of the shock waves in nonplanar geometries differs significantly from the planar geometry due to the presence of ν/τ term in Eq. (18). If we increase $\mid \tau \mid$ to very large values, the nonplanar

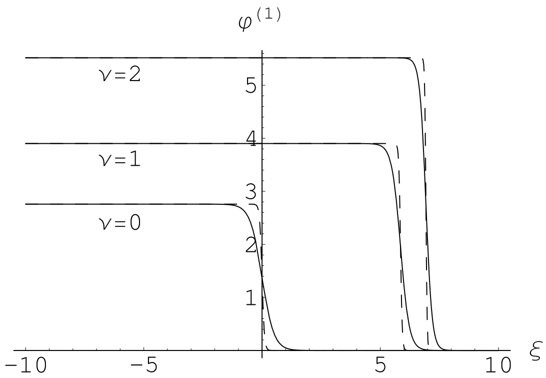

Figure 1. Nonlinear shock waves are shown in different geometries at $\tau = -5$ for two values of η_0, the viscosity parameter, where $\alpha = 0.5$, $\mu = 0.4$ (solid line for $\eta_0 = 0.5$, dashed line for $\eta_0 = 0.1$).

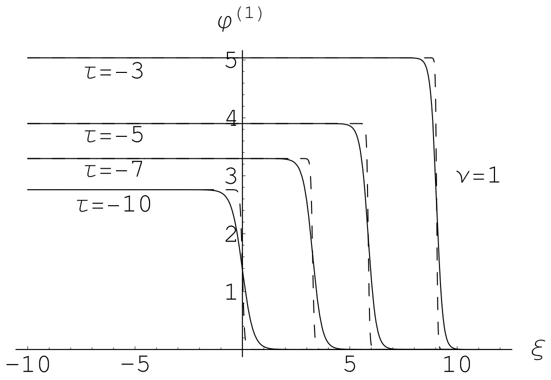

Figure 2. Variation in $\phi^{(1)}$ with respect to ξ at different values of τ for two values of η_0, where $\nu = 1$, and the other parameters being same as those in Figure 1 (solid line for $\eta_0 = 0.5$, dashed line for $\eta_0 = 0.1$).

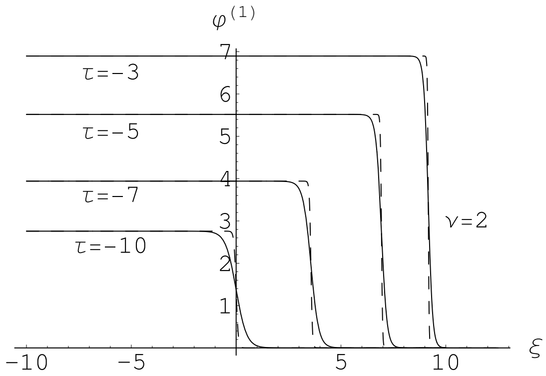

Figure 3. Variation in $\phi^{(1)}$ with respect to ξ at different values of τ for two values of η_0, where $\nu = 2$, and the other parameters being same as those in Figure 1 (solid line for $\eta_0 = 0.5$, dashed line for $\eta_0 = 0.1$).

geometries would approach the planar geometry. It has been also found that the height of the shock wave remains unchanged but steepness of the shock wave increases as η_0, the viscosity parameter decreases. In Figures 2 and 3, the effects of kinematic viscosity in both cylindrical and spherical geometries are investigated respectively for several values of τ. It is found that as the magnitude of τ increases the shock height and steepness decreases and the effect is more pronounced in spherical by comparison with the cylindrical geometry. Figure 4 explores the change in shock wave structure due to the variation of α in the cylindrical geometry. It is found that decrease in α, the ratio of ion and electron temperature enhances the amplitude as well as the steepness of the shock front. It is worth mentioning here that the increase in steepness tells us that the

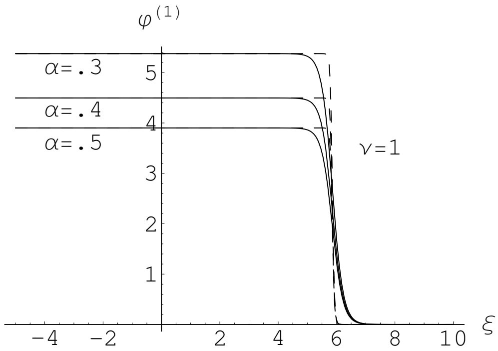

Figure 4. Cylindrical shock profile at $\tau = -5$ for several values of α and for two values of η_0, where the other parameters being same as those in Figure 1 (solid line for $\eta_0 = 0.5$, dashed line for $\eta_0 = 0.1$).

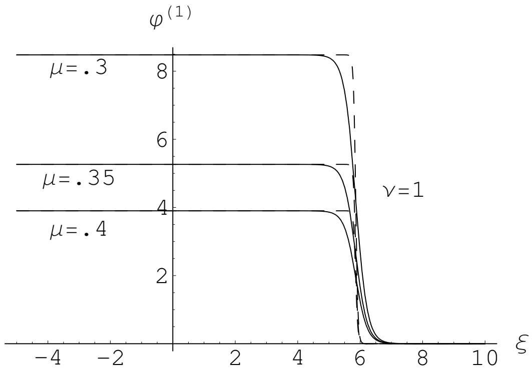

Figure 5. Cylindrical shock profile at at $\tau = -5$ for several values of μ and for two values of η_0, where the other parameters being same as those in Figure 1 (solid line for $\eta_0 = 0.5$, dashed line for $\eta_0 = 0.1$).

change in parameters downstream of the shock is drastic while the amplitude of the shock determines its strength. The solution of equation (18) is depicted in Figure 5 for several values of μ and for two values of η_0 in cylindrical geometry. It is seen that the height of the shock wave decreases with μ. The solution of the ordinary differential equations (21) and (22) is done numerically in Figure 6 and in Figure 7, respectively for two values of η_0, the viscosity parameter, assuming $v \to 0$, $\dfrac{dv}{d\eta} \to 0$ as $\eta \to 0$.

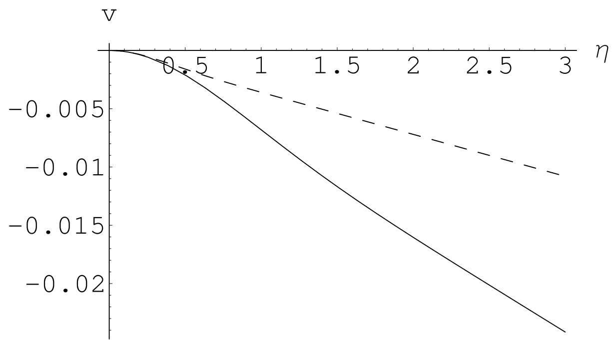

Figure 6. Plot of v *vs.* η for the numerical solution of the ordinary differential equation (21) for two values of η_0, where $C = \eta_0/2$ (solid line for $\eta_0 = 0.5$, dashed line for $\eta_0 = 0.1$).

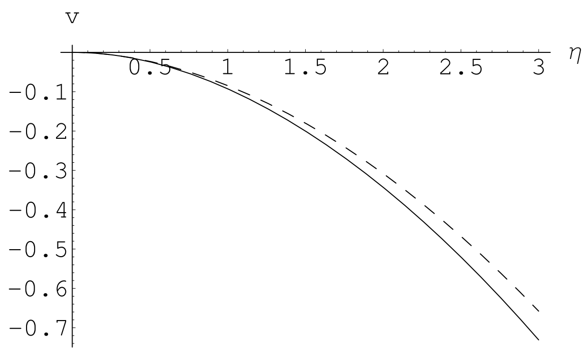

Figure 7. Plot of v *vs.* η for the numerical solution of the ordinary differential equation (22) for two values of η_0, where $C = \eta_0/2$ (solid line for $\eta_0 = 0.5$, dashed line for $\eta_0 = 0.1$).

4 Conclusion

Burgers' equations for dust ion acoustic waves in an adiabatic dusty plasma are numerically investigated in nonplanar cylindrical and spherical geometry. In this paper we have investigated nonplanar cylindrical and spherical DIASWs in an adiabatic dusty plasma. The dependence of the DIASWs on various plasma parameters is explored in detail. The numerical results reveal the differences between the cylindrical DIASW, spherical DIASW and one-dimensional DIASW. It is found that the shock strength is maximum for the spherical geometry, intermediate for cylindrical geometry, while it is minimum for the planar geometry. It is observed that the propagation characteristics of shock waves in nonplanar geometries differ significantly from the planar geometry due to the presence of

ν/τ term in Eq. (18). The temporal evolution of the DIASW in cylindrical and spherical geometry is explored and the results are discussed from the numerical stand point. Finally, it is shown that if we increase τ to large negative values, the nonplanar geometries would approach the planar geometry.

References

[1] D.A. Mendis, M. Rosenberg (1994) *Ann. Rev. Astron. Astrophys.* **32** 419.
[2] M. Horanyi, D.A. Mendis (1986) *J. Geophys. Res*. **91** 355.
[3] P.K. Shukla (2001) *Phys. Plasmas* **8** 1791.
[4] M. Horanyi, D.A. Mendis (1985) *Astrophys. J*. **294** 357.
[5] C.K. Goertz (1989) *Rev. Geophys*. **27** 271.
[6] T.G. Northrop (1992) *Phys. Scr.* **45** 475.
[7] D.A. Mendis, M. Rosenberg (1992) *IEEE Trans. Plasma Sci*. **20** 929.
[8] F. Verheest (1996) *Space Sci. Rev*. **77** 267.
[9] J.C. Johnson, N. D'Angelo, R.L. Merlino (1990) *J. Phys. D* **23** 682.
[10] N. D'Angelo (1995) *J. Phys. D* **28** 1009.
[11] P.K. Shukla, V.P. Silin (1992) *Phys. Scr*. **45** 508.
[12] Y. Nakamura, H. Bailung, P.K. Shukla (1999) *Phys. Rev. Lett*. **83** 1602.
[13] Y. Nakamura (2002) *Phys. Plasmas* **9** 440.
[14] P.K. Shukla (2000) *Phys. Plasmas* **7** 1044.
[15] P.K. Shukla, A.A. Mamun (2002) *IEEE Trans. Plasma Sci*. **30** 720.
[16] P.K. Shukla, A.A. Mamun (2003) *New. J. Phys*. **5** 171.
[17] A. Rahman, Fatema Sayed, A.A. Mamun (2007) *Phys. Plasmas* **14** 034503.
[18] A.A. Mamun, P.K. Shukla (2002) *Phys. Plasmas* **9** 1468.
[19] X. Jukui, L. He (2003) *Phys. Plasmas* **10** 339.
[20] J.-K. Xue (2003) *Phys. Lett. A* **314** 479.
[21] J.-K. Xue (2003) *Phys. Plasmas* **10** 3430.
[22] J.-K. Xue (2005) *Phys. Plasmas* **12** 012314.
[23] S. Maitra, R. Roychoudhury (2003) *Phys. Plasmas* **10** 2230.
[24] CRC Handbook of Lie Group Analysis of Differential Equations, Vol.1, Edited by N.H. Ibragimov (CRC Press, Ann Arbor, 1993), P-194.